Protective effect of resveratrol in di-n-butyl phthalate-induced nephrotoxicity: Immunohistochemical and ultrastructural studies

Article · January 2017

CITATIONS
0

READS
173

6 authors, including:

Cigdem Elmas
Gazi University
95 PUBLICATIONS **793** CITATIONS
SEE PROFILE

C.Merve Seymen
Gazi University
33 PUBLICATIONS **42** CITATIONS
SEE PROFILE

Dila Şener
Bahçeşehir University
5 PUBLICATIONS **2** CITATIONS
SEE PROFILE

Güleser Göktaş
Lokman Hekim Üniversitesi Tıp Fakültesi
32 PUBLICATIONS **228** CITATIONS
SEE PROFILE

Protective Effect of Resveratrol in Di–n-butyl Phthalate–Induced Nephrotoxicity

Immunohistochemical and Ultrastructural Studies

Cigdem Elmas, Ph.D., **Cemile Merve Seymen,** Ph.D., **Dila Sener,** Ph.D., **Güleser Göktas,** Ph.D., **Tayfun Göktas,** M.D., and **Ayten Türkkanı,** M.D.

OBJECTIVE: To explore the renoprotective nature of resveratrol by assessing markers of antioxidant competence in di–n-butyl phthalate (DBP)–injured rat kidneys with immunohistochemistry and electron microscopic techniques and as well as biochemical analyses.
STUDY DESIGN: A total of 36 adult female 20-day-old Wistar albino rats were given a diet containing either 500 mg/kg/day DBP (low-dose group) or 1,000 mg/kg/day DBP (high-dose group) dissolved in corn oil for 4 weeks. To study the potential protective effects of resveratrol and the effects of a solvent for resveratrol, other groups were used as controls and were given a solvent (carboxymethyl cellulose [CMC], 10 mL/kg), 500 mg/kg/day DBP+20 mg/kg/day resveratrol, or 1,000 mg/kg/day DBP+20 mg/kg/day resveratrol.
RESULTS: DBP and CMC treatment increased renal lipid peroxidation significantly and decreased the RSH level. TEM and SEM results showed degenerative changes such as deletion, folding and thickening of basement membrane, appearance of electron-dense intramembranous and mesangial deposits, and deletion of foot processes in the high-dose DBP-treated group. Treatment with resveratrol led to an improvement in both biochemical and histological alterations induced by DBP or CMC. Immunohistochemical results also supported our electron microscopic findings.
CONCLUSION: DBP caused renal toxicity by inducing lipid peroxidation and morphological alterations, and resveratrol protects against DBP-induced nephrotoxicity. (Anal Quant Cytopathol Histpathol 2017; 39:17–34)

Keywords: butyl phthalate, CASP3, Caspase-3, di-n-butyl phthalate, ET1 protein, kidney, resveratrol, scanning transmission electron microscopy tomography, TEM tomography, transmission electron microscopy.

Di–n-butyl phthalate (DBP) is a phthalic acid ester (PAE) that is used as a plasticizer for elastomers such as polyvinyl, and in recent years DBP has been considered as one of the contaminants that

From the Departments of Histology and Embryology and of Physiology, Faculty of Medicine, Gazi University, and the Department of Histology and Embryology, Faculty of Medicine, TOBB University of Economics and Technology, Ankara, Turkey.

Dr. Elmas is Professor, Department of Histology and Embryology, Faculty of Medicine, Gazi University.

Dr. Sener is Assistant Professor, Department of Histology and Embryology, Faculty of Medicine, Gazi University.

Dr. Seymen is Research Assistant, Department of Histology and Embryology, Faculty of Medicine, Gazi University.

Dr. G. Göktas is Specialist, Department of Histology and Embryology, Faculty of Medicine, Gazi University.

Dr. T. Göktas is Specialist, Department of Physiology, Faculty of Medicine, Gazi University.

Dr. Turkkani is Associate Professor, Department of Histology and Embryology, Faculty of Medicine, TOBB University of Economics and Technology.

Address correspondence to: Ayten Türkkanı, M.D., Department of Histology and Embryology, First Floor, Building of the Academic Deanship, Faculty of Medicine, TOBB University of Economics and Technology, 06560 Ankara, Turkey (aytenturkkani@gmail.com).

Financial Disclosure: The authors have no connection to any companies or products mentioned in this article.

0884-6812/17/3901-0017/$18.00/0

organisms are exposed to through environmental contamination as a result of human activities. PAEs have worldwide uses in plastics, coating, and the cosmetic industry, and they are classified in the synthetic endocrine disruptor group.[1] Besides its wide use in industry, DBP is used as a plasticizer and solvent. As a plasticizer DBP is used mainly for nitrocellulose-polyvinyl acetate and polyvinyl chloride, aerosol valve lubricator, antifoam agents, skin conditioning agent, plasticizer nail varnish, nail extender, and hair spray.[2] In addition, as DBP is used on a whole range of products, from children's toys to drinking water, it is a low-level contaminant used on a wide scale in the environment. As a consequence of this widespread use, release of phthalates into the environment occurs during production, usage, and disposal stages due to their low molecular weight, and they have irreversible binding on the polymer matrix. It has been reported that at concentrations below water solubility values, phthalates induced acute and chronic toxicity for water and soil organisms, and their rising toxic effects depends on increased solubility. Some forms are known as suspected mutagens and carcinogens. Phthalates have been reported to be harmful to human health and the environment by the U.S. Environmental Protection Agency, and they have been put on the list of priority pollutants.[3]

Moreover, DBP affects apoptosis, causes degeneration in many tissues, and destroys the tissues by reducing glutathione (GSH) and/or total sulphydryl group (RSH) levels.[4] Destruction of the renal tissues such as glomerules and tubules immediately affects renal functions and leads to permanent renal insufficiency.[5] In a previous study it was indicated that accumulation of DBP in kidney tissue with dietary high intake leads to increasing kidney weight in females, DBP-associated formation of radioactivity in many organs, cyst formation in the kidney, and renal peroxisome proliferation.[6] Histopathological studies that include the effects of DBP on kidney tissue are limited, while more studies have been carried out on PAEs and the other isoforms.

Many antioxidants have been described to reduce the side effects of DBP, like harmful chemicals on renal functions. Resveratrol is a polyphenolic phytoalexin that occurs naturally in many plant species, including grapevines and berries, and exhibits an abundance of pharmacologic health benefits including antioxidant, antimutagenic, anti-inflammatory, estrogenic, antiplatelet, anticancer, and cardioprotective properties.[7] Recently, resveratrol has been reported to possess protective effects in kidneys.[8] In many studies resveratrol has been shown to (1) improve glycerol-stimulated renal damage by inhibiting lipid peroxidation and suppressing the inflammatory process,[9] (2) decrease renal dysfunction occurring after ischemia/reperfusion injury,[10] (3) partially reduce sepsis-induced renal damage by balancing oxidant-antioxidant status,[11] and (4) reduce cisplatin-induced structural and functional renal changes via decreasing the amount of free radicals and inhibiting inflammatory cell infiltrates.[12] However, a detailed literature review did not identify any studies that explored the protective effects of resveratrol against DBP-induced damage in kidney tissue with combined electron microscopic, biochemical, and immunohistochemical methods.

Various signaling molecules are recognized in the kidney to indicate apoptosis and degeneration. Among them, caspase 3 is a frequently activated death protease, catalyzing the specific cleavage of many key cellular proteins and having a central role in the execution of apoptosis.[13] It has been reported that caspase 3 expression is weak in normal kidney tissue, but expression increases during exposure to different chemicals in renal tissue.[14,15] Moreover, endothelin-1 (ET-1), a 21-amino acid secretory protein synthesized in vascular endothelial cells, is a potent vasoconstrictor and plays a fundamental physiological role in maintenance of blood pressure in humans. It is also normally expressed mostly in distal and proximal tubules of kidney tissues, besides the vasculer structures, but its overexpression was reported in many tissues, including in the kidney, in degenerative conditions.[16]

In our study we aimed to investigate the efficacy of resveratrol against the potential damages that would appear in the kidney tissue due to administration of DBP by evaluating total sulphydryl groups (RSH) and lipid peroxidation (LPO) values biochemically, assessing caspase 3 and ET-1 signaling molecules immunohistochemically and with transmission electron microscope (TEM) and scanning electron microscope (SEM) ultrastructurally.

Materials and Methods

Chemicals

Di–n-butyl phthalate (98.0% purity, 278.34 g/Mol, lot sze8149x,) and resveratrol (99% purity, 228.24 g/Mol, lot 038k5202) were purchased from Sigma-Aldrich (St. Louis, Missouri, USA). Resveratrol was

stored at 2–4°C and protected from sunlight. Solvent carboxymethyl cellulose, sodium salt (CMC, $C_{28}H_{30}Na_8O_{27}$, lot 03820 kh) was obtained from Sigma-Aldrich. All other chemicals were of analytical grade and were obtained from standard commercial suppliers.

Animals

Twenty-day-old female Wistar Albino rats (Gazi Universty Medical School Experimental Animal Breeding and Experimental Research Center, Ankara, Turkey) were used in this research. Wistar rats weighing 30–40 g were housed in clean, sterile, polypropylene cages under standard vivarium conditions (12 h light/dark cycles) with access to water and standard rat chow (Korkutelim Yem Ltd., Antalya, Turkey) with a composition 41% fat, 12% water, 25% protein, 7% cellulose, 8% total ash, 2% inorganic ash, 1% NaCl, 1–1.8% calcium, 0.9% phosphore, 0.5–0.8% sodium, 1% lysine, and 0.3% methionine with adequate mineral and vitamin levels for the animals. The animals were housed 6 per cage in an air-conditioned animal room at 22±3°C and 55±10% humidity. Animal experiments were premeditated and executed in accordance with the ethical norms approved by Institutional Animal Ethics Committee Guidelines (Approval No. 09.069). The animals were acclimatized to the laboratory conditions for 4 weeks prior to the inception of experiments.

Experimental Design

After 7 days of acclimation to the environment, rats were divided into 6 groups (n=6 animals per group). Group I served as a control, receiving saline throughout the experimental period. Group II received 500 mg/kg DBP in 1 mL/kg corn oil once a day, taken daily by oral gavage for 4 weeks. Group III rats received 1000 mg/kg DBP in 1 mL/kg corn oil once a day for 4 weeks and taken daily by oral gavage.[17] Group IV received only solvent CMC (10 mg/kg body weight) once a day for 4 weeks taken daily by oral gavage during the experimental period. Group V received 500 mg/kg DBP in 1 mL/kg corn oil plus resveratrol (20 mg/kg body weight) dissolved in CMC taken daily by oral gavage for 4 weeks.[18] Group VI received 1000 mg/kg DBP in 1 mL/kg corn oil plus resveratrol (20 mg/kg body weight) dissolved in CMC taken daily by oral gavage for 4 weeks. Based upon previous studies which showed that corn oil had no harmful effect on renal tissue, we did not establish a corn oil group within our experimental groups.[19] All gavage applications were done at 9:00 am. At the end of the 4-week experimental period, tissue samples were collected under ketamine (45 mg/kg) and xylazine (5 mg/kg) anesthesia. Kidney tissues were removed, some of them stored at –80°C and some of them taken into the fixatives for pending analysis.

Preparation of Kidney Tissue

Kidney tissues from control and experimental groups of rats were taken immediately after sacrificing the animals, shortly washed in physiological saline, and taken into a neutral formaldehyde and glutaraldehyde for fixation.

Transmission Electron Microscopic Study

A portion of kidney (about 1 mm^3) from the control and experimental rat groups was fixed in 3% glutaraldehyde in 200 mM sodium phosphate buffer (pH 7.4) for 3 hours at 4°C. Tissue samples were washed with the same buffer and postfixed in 1% osmium tetroxide and 200 mM sodium phosphate buffer (pH 7.4) for 1 hour at 4°C. The samples were again washed with the same buffer for 3 hours at 4°C, dehydrated with graded series of ethanol, and embedded in Araldite. Thin sections were cut with Leica EMUC7 ultramicrotome using a diamond knife (Leica EMUC7, Vienna, Austria), mounted on a copper grid and stained with 2% uranyl acetate and lead citrate. The grids were examined under a Carl Zeiss EVO LS 10 TEM-SEM microscope (Germany). A total number of 4 cortical kidney tissues were investigated from each group.

Scanning Electron Microscopic Study

Segments about 1 mm^3 were prepared by microdissection with a stereoscope from the cortex of the kidneys. Tissue samples were fixed with 2.5% phosphate-buffered glutaraldehyde solution at room temperature for 2 hours, and then pieces were immersed in distilled water for 20 minutes and 3 times for each rinse. Following this, a secondary fixation was performed using 1–4% osmium tetroxide in distilled water at room temperature for 2 hours, then rinsed again 3 times in distilled water. Samples were placed in increasing degrees of ethanol ranges for dehydration. Tissues were subsequently dried with critical point drying apparatus (EM CPD030, Leica), and dehydration was completed. After this drying process using liquid silver, each specimen was mounted with sil-

ver paste and coated with gold-palladium alloy in coating apparatus (LLC Desk V sputter/etch unit; Denton Vacuum). Finally, tissues were inserted in holders of Carl Zeiss EVO LS 10 TEM-SEM microscope. The investigation was made using an SEM microscope, and photographs were taken. A total number of 6 cortical kidney tissues were investigated from each group.

Immunohistochemical Study

Kidney tissue samples obtained from the study groups were fixed in 10% neutral formalin for about 72 hours. They were dehydrated in an increasing series of ethanol and were paraffin-embedded for conventional histological diagnosis. Cross sections (5 μm) were mounted on polylysin-coated slides (Menzer-Glaser, Braunschweig, Germany), deparaffinized with xylene, and rehydrated. The slides were kept in a microwave oven in citrate buffer (LabVision, Fremont, California, USA) for heat-induced antigen retrieval through microwave irradiation so as to increase the sensitivity of immunohistochemical detection. Endogenous peroxidase activity was blocked with 3% hydrogen peroxide (Fisher Scientific, Melrose Park, Illinois, USA) for 15 minutes and washed 2 times in phosphate-buffered saline solution (PBS Pack, Cat. no. 00–3000 Zymed, San Francisco, California, USA). The epitopes were stabilized by application of serum-blocking solution (ThermoScientific, Fremont, California, USA) and were divided into groups by slides. The slides were incubated with polyclonal primary antibodies of caspase 3 (Neomarkers, Fremont, California, USA) and ET-1 (N-8, sc-21625; Santa Cruz Biotechnology, USA) for 60 minutes at room temperature. After that, the biotinylated secondary antibody (ThermoScientific) was applied. Thereafter, streptavidin peroxidase (ThermoScientific) was applied to the slides, and AEC (ThermoScientific) was used as a chromogen. Afterwards, all slides were counterstained with Mayer's hematoxylin. Slides were examined with photolight microscope (DM4000B Image Analyze System, Leica) and Leica DFC280 plus camera. The number of immune-positive cells were measured manually by using the Qwin software program in consecutive areas for serial cutaways taken from all animals and all groups. The following semiquantitative scoring system was used to assess the immunolabeling intensity: 0=no staining, 1=weak, 2=moderate to weak, 3=moderate, 4=moderate to strong, and 5=strong labeling. Two independent observers who were blind to the treatment protocol performed the immunolabeling score evaluations independently. The H-score was calculated using the following equation:

$$\text{H-score} = \sum \text{Pi}\,(i+1),$$

where i is the intensity of caspase 3 and ET1 labeling with a value of 0, 1, 2, 3, 4, 5, and Pi is the percentage of labeled cells for each intensity, varying from 0–100%.[20] Results were expressed as the mean ± SD.

Malondialdehyde (MDA) and Total Sulphydryl Group (RSH) Assays

Lipid peroxidation was quantified by measuring the formation of thiobarbituric acid–reactive substances (TBARS), as described previously by Kurtel.[21] Aliquots (0.5 mL) were centrifuged and the supernatants were added to 1 mL of a solution containing 15% (wt/vol) tricarboxylic acid, 0.375% (wt/vol) thiobarbituric acid, and 0.25 N HCl. Protein precipitate was removed by centrifugation, and the supernatants were transferred to glass test tubes containing 0.02% (wt/vol) butylated hydroxytoluene to prevent further peroxidation of lipids during subsequent steps. The samples were then heated for 15 minutes at 100°C in a boiling water bath, cooled, and centrifuged to remove the precipitate. The absorbance of each sample was determined at 532 nm. Lipid peroxide levels were expressed in terms of TBARS equivalents using an extinction coefficient of $1.56 \times 105\ \text{mol}^{-1}$.

The RSH levels were determined by the method of Kurtel[21]: 0.5 mL of each sample was mixed with 1 mL of a solution containing 100 mM Tris-HCl (pH 8.2), 1% sodium dodecyl sulfate, and 2 mM EDTA. The mixture was incubated for 5 minutes at 25°C and centrifuged to remove any precipitant. Then 5,5-dithiobis (2-nitrobenzoic acid)/DTNB 0.3 mM was added to each reaction volume and incubated for 15 minutes at 37°C. The absorbance of each sample was determined at 412 nm.[21]

Statistical Analysis

Data analysis was performed using Statistical Package for the Social Sciences (SPSS) version 15.0 software (SPSS Inc., Chicago, Illinois, USA). Results were shown as mean and standard deviation. Groups were compared using Kruskal-Wallis H test. When Kruskal-Wallis test results were significant, Bonferroni's adjusted Mann-Whitney U test was used for pairwise comparisons. The Friedman

test was used to compare within group measurements. Bonferroni's adjusted Wilcoxon signed-rank test was used to determine which measurement differs from which one. A value of $p<0.05$ was considered statistically significant.[22]

Results

Transmission Electron Microscopic Results

Group I (Control Group). Ultrastructurally the capillary loops, mesangial cells, endothelial cells, glomerular basement membrane (GBM), podocyte, primary and secondary foot processes were observed to be normal. Podocytes are situated between glomerular capillaries, and their secondary foot processes were extended and rest on the basement membrane. Numerous filtration slit membranes were observed between the processes of glomerular capillaries (Figure 1A).

Group II (Low-Dose DBP-Treated Group). In the low-dose DBP-treated animals most of the renal corpuscules were slightly affected. There were large vacuoles and electron-dense inclusions in different kinds of cells in the corpuscule. GBM showed obvious thickening on deletion in different sites of the same glomeruli. Intramembranous and mesangial electron-dense deposits were noticed. Podocyte foot process effacement was also observed (Figure 2A).

Group III (High-Dose DBP-Treated Group). Deletion, thickening and curling of GBM, presence of electron-dense inclusions in the cytoplasm of nearly all kinds of cells in glomeruli, primary and secondary foot effacement, intramembranous and mesangial electron-dense deposits were the most evident degenerative findings in the higher-dose DBP-treated group (Figure 3A).

Group IV (Carboxymethyl Cellulose, Solvent). Carboxymethyl cellulose (CMC)–treated animals also showed very conspicuous degenerative alteration ultrastructurally. Membranous inclusions and foam-like vacuoles were observed in endothelial cytoplasm of capillary loops. Intramembranous electron-dense deposits, deletion and thickening of GBM were also noticed. Most of the secondary foot processes of podocytes appeared flattened and amalgamated with each other with complete disappearance of their slit membranes (Figure 4A).

Group V (Low-Dose DBP+Resveratrol). Combined treatment with low-dose DBP and resveratrol led to improvement in the ultrastructure of the kidney,

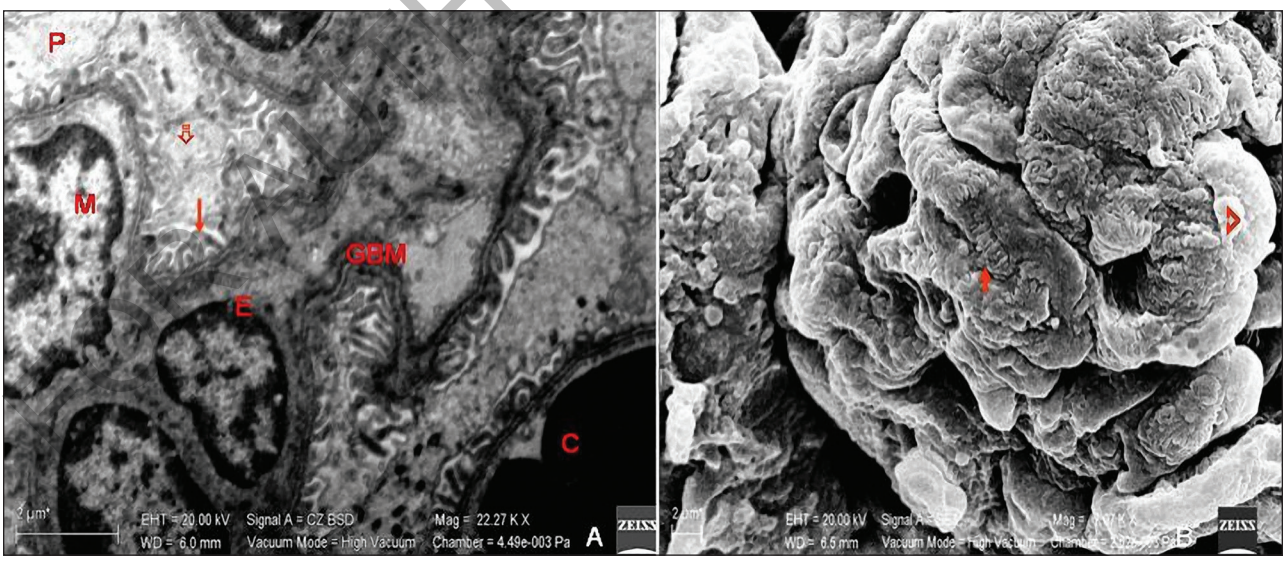

Figure 1 (A) Transmission electron microscope (TEM). Capillary loops (C), mesangial cells (M), endothelial cells (E), glomerular basement membrane (GBM), podocyte (P), and primary (⇧) and secondary (↓) foot processes are seen in their normal appearance (uranyl acetate, lead citrate). (B) Scanning electron microscope (SEM) micrograph of glomerular podocytes are seen. The large cell body (▷) sends out thick primary processes that further branch into fine secondary (foot) processes (▲) that interdigitate with foot processes from adjacent podocytes.

Figure 2 A) TEM. Intramembranous (⇈) and mesangial (➡) electron-dense deposits, podocyte (P) foot process effacement (↘), deletion (➲) and thickening (✱) of GBM, large vacuoles (V), electron-dense inclusions (➴), capillary loops (C), mesangial cells (M), and endothelial cells (E) are seen (uranyl acetate, lead citrate). (B) Scanning electron microscopy of the low-dose group. Glomeruli showing prominent cell bodies (➧) and a small amount of precipitated phthalate crystal deposits (↘) were observed under SEM in animals of the low-dose group. Normal-shaped erythrocytes (Er) are seen between the capillary loops, as well as foot process effacement.

which appeared nearly similar to that of the control, but there were still some degenerative findings in some of the glomeruli. For example, mesangial and intramembranous electron-dense deposits were still seen in some places in the corpuscles. Large vacuoles and myelin-like figures in vacuoles

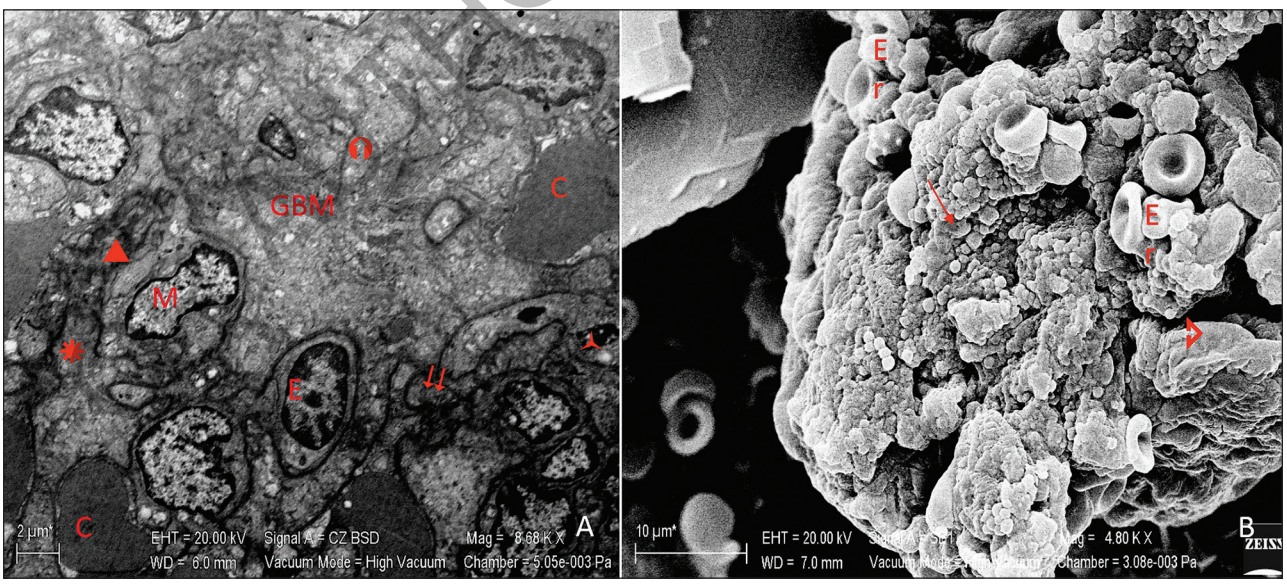

Figure 3 (A) TEM. Lysosomal electron-dense inclusions (➴), deletion (➲), curling (▲) and thickening (✱) of GBM, capillary loops (C), mesangial cells (M), endothelial cells (E), intramembranous (⇈) and mesangial (➡) electron-dense deposits are seen (uranyl acetate, lead citrate). (B) SEM. Glomerulus in the high-dose DBP group showing distorted shapes of erythrocytes (Er) which were not typical biconcave discs under normal blood flow conditions; large deposits of precipitated phthalate crystals (↘) are seen. Partial distortion in podocyte shape can be seen (➧) also.

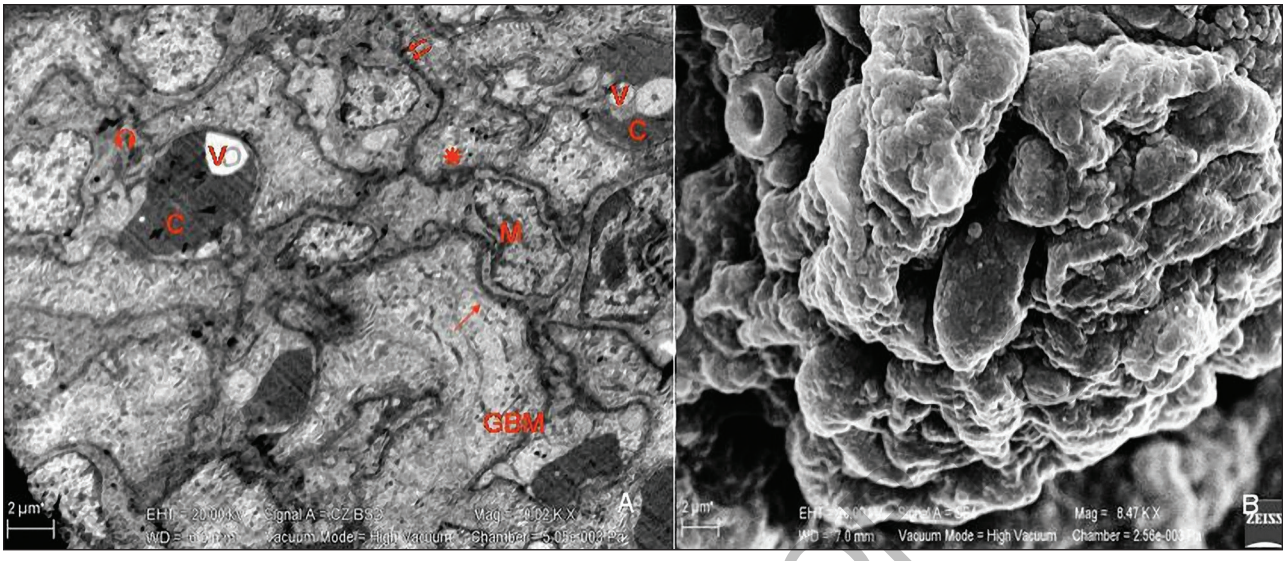

Figure 4 (A) TEM. Capillary loops (C), mesangial cells (M), glomerular basement membrane (GBM), vacuoles (V), intramembranous (⇈) electron-dense deposits, deletion (➲) and thickening (✱) of GBM, and foot process effacement (↘) (uranyl acetate, lead citrate). (B) SEM. Kidney glomerulus in the solvent (CMC) group showing distorted shapes of podocyte cells (➧) with their distorted primary and secondary (foot) processes, but there are no deposits of precipitated crystals. Primary and secondary foot processes are not clearly seen.

were noticed in the capillary loops and cytoplasm of mesangial and endothelial cells also. There were electron-dense inclusions in the primary processes of podocytes (Figure 5A). On the other hand, podocytes and their primary and secondary processes were clearly seen when compared with group III ($p<0.05$).

Group VI (High-Dose DBP+Resveratrol). Combined treatment with high-dose DBP and resveratrol had more severe degenerative findings than group 5 ultrastructurally ($p<0.05$). Intramembranous and mesangial electron-dense deposits were conspicuous. Vacuoles with myelin-like figures in capillary loops and membranous vacuoles in mesangial cell cytoplasm were noticed (Figure 6A). Additionally, effacement in the foot process was evident. Beside these degenerative findings, favorable effects of resveratrol in the ultrastructure of the glomeruli were observed in many places when this group was compared with groups II and III. Degeneration criteria of TEM findings are summarized in Table I; mean of degeneration criteria in TEM is presented in Figure 7.

Scanning Electron Microscopic Results

Group I. Scanning electron microscope (SEM) micrograph of glomerular structures appeared normal in the control group. The large cell body of podocytes sent out thick primary processes that further branch into fine secondary (foot) processes that interdigitate with foot processes from adjacent podocytes. The surface contours of foot processes of podocytes were smooth and tightly opposed each other, and filtration slits were also narrow and seen in their normal appearance in SEM (Figure 1B).

Group II. The low-dose DBP-treated group had a small amount of precipitated phthalate crystals around podocytes and capillary loops. Foot process effacement was very prominent. Erythrocytes appeared normal. Distortion in the shape of some podocytes was present (Figure 2B).

Group III. Degenerative findings that were seen in group II were more conspicuous in the high-dose DBP-treated group in SEM ($p<0.05$). This group had more abundant precipitated phthalate crystals, and foot process effacement was also more prominent ($p<0.05$). The cell body of the podocytes was not clearly seen because the phthalate crystal accumulation and detectable podocyte cell bodies had prominent distortion in their shape. Distortion in the shape of erythrocytes was also apparent in this group (Figure 3B).

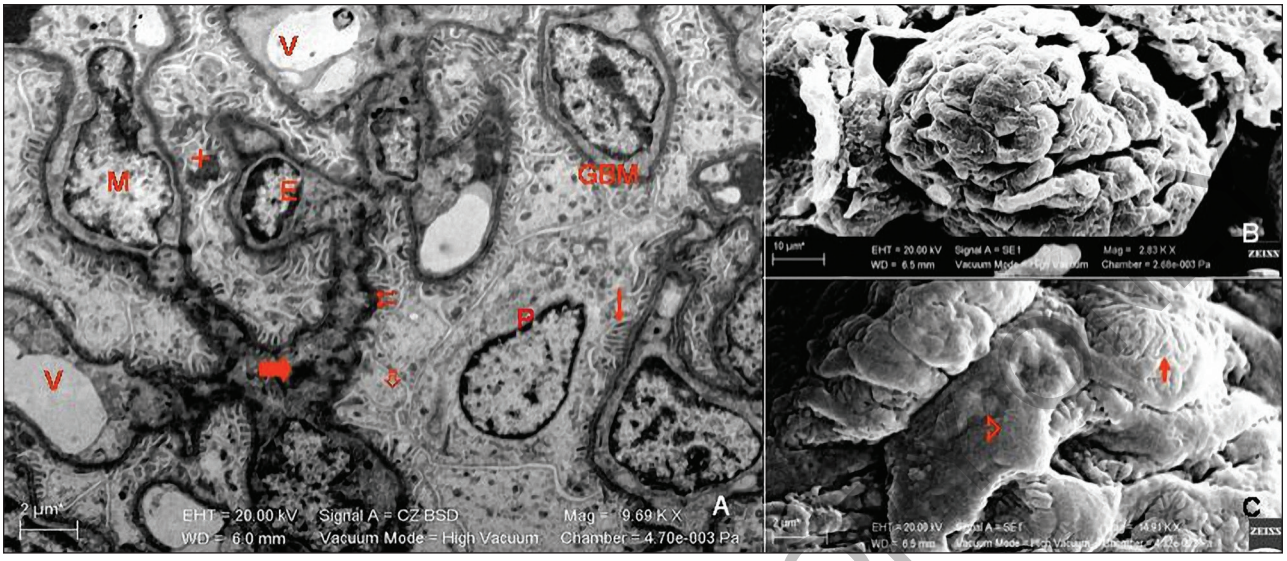

Figure 5 (A) TEM. Mesangial cells (M), podocytes (P), endothelial cells (E), glomerular basement membrane (GBM), myelin-like figures in vacuoles (V), intramembranous (⇈) and mesangial (➡) electron-dense deposits, filtration slits (↘), primary (⇪) and secondary (⇂) foot processes, and electron-dense inclusions in the primary process of podocytes (+) (uranyl acetate, lead citrate). (B) SEM image of a kidney glomerulus demonstrating the glomerulus with normal appearance of a cluster of capillary loops. The capillaries are covered by podocytes (⏵) that form fine slits (⏶) on the outside surface of the capillary wall.

Group IV. The most remarkable and constant change of the solvent (CMC) group was the distortion in the shape of the podocyte as compared with the other experimental groups ($p<0.05$). Fil-

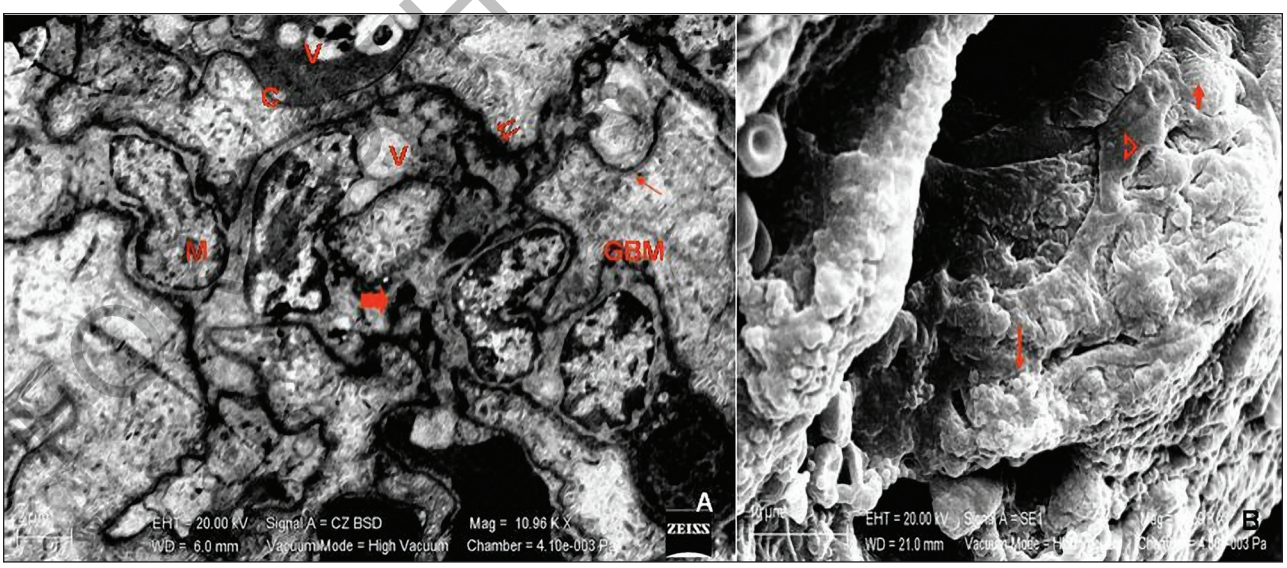

Figure 6 (A) TEM. Mesangial cells (M), glomerular basement mebrane (GBM), large vacuoles and electron-dense core material in the vacuoles (V), intramembranous (⇈) and mesangial (➡) electron-dense deposits, vacuoles in the capillary loop (C), and foot process effacement (↘) (uranyl acetate, lead citrate). (B) SEM. Deposits of precipitated phthalate crystals are seen in some spaces (↘), distorted shapes of podocyte cells (⏵) with their distorted primary and secondary (foot) processes are seen (⏶), and the urinary space between the capillary loops is not seen well.

Table I *Degeneration Criteria in TEM*

Degeneration criterion	Group 1	2	3	4	5	6	p Value
Electron-dense intramembranous deposits	0.00 ± 0.00^{a}	2.00 ± 0.82^{b}	2.25 ± 0.50^{b}	2.00 ± 0.00^{b}	1.00 ± 0.82^{b}	1.75 ± 0.50^{b}	0.009
Electron-dense mesangial deposits	0.75 ± 0.50^{a}	3.00 ± 0.82^{b}	$2.00\pm0.00^{b,c}$	3.00 ± 0.82^{b}	$1.00\pm0.00^{a,c}$	$1.75\pm0.50^{a,c}$	0.002
Foot process effacement	0.00 ± 0.00^{a}	3.00 ± 0.82^{b}	4.75 ± 0.50^{c}	1.00 ± 0.00^{d}	$2.00\pm1.41^{b,d}$	3.00 ± 0.00^{b}	0.001
Inclusions	0.25 ± 0.50^{a}	1.75 ± 0.50^{b}	2.00 ± 0.00^{b}	2.25 ± 0.50^{b}	$1.00\pm0.00^{a,c}$	$1.75\pm1.26^{b,c}$	0.011
Large vacuoles	0.00 ± 0.00^{a}	2.00 ± 0.00^{b}	0.25 ± 0.50^{a}	4.00 ± 0.82^{c}	0.75 ± 0.50^{a}	0.75 ± 0.50^{a}	0.001
GBM thickening	0.00 ± 0.00^{a}	2.00 ± 0.82^{b}	$0.75\pm0.50^{a,c}$	2.00 ± 0.00^{b}	$0.75\pm0.50^{a,c}$	$1.00\pm0.00^{b,c}$	0.002
GBM curling	0.25 ± 0.50^{a}	0.25 ± 0.50^{a}	4.00 ± 0.82^{b}	0.25 ± 0.50^{a}	0.00 ± 0.00^{a}	2.00 ± 0.00^{c}	0.002
GBM deletion	0.00 ± 0.00^{a}	2.00 ± 0.82^{b}	$3.00\pm0.82^{b,c}$	0.25 ± 0.50^{a}	$1.25\pm0.96^{a,b}$	$0.75\pm0.50^{a,b}$	0.004

Data are given as mean±standard deviation.
[a,b,c]The difference between the averages indicated by different letters are statistically significant, while the difference between the averages indicated by the same letters are not statistically significant ($p<0.05$).

tration slits were not recognized clearly because of the presence of foot process effacement. Crystalloid structures were not present (Figure 4B).

Groups V and VI. The low-dose DBP+resveratrol group showed very remarkable improvement in the SEM. Only rarely was foot process effacement seen, and these were detected in only a few glomeruli (Figure 5B). On the other hand, high-dose DBP+resveratrol group SEM findings were very similar to those of group II (Figure 6B) ($p<0.05$). Degeneration criteria of SEM findings are summarized in Table II.

Immunohistochemical Results

The renal cortex from all of the experimental and control rats were examined with light microscope. The section of renal cortex was assessed for the immunohistochemistry of antibodies in proximal and distal tubules, glomeruli, and endothelial cells of capillaries.

Caspase 3 Immunostaining

Immunohistochemistry was done for the detection of apoptosis in the kidney by using polyclonal antibodies against caspase 3 antigen, which is expressed during the last stages of apoptosis. The site where the red color develops indicates the presence of antigen.

Group I. Immunostaining was detected mostly in distal tubules. There was mild immunostaining in distal tubules, whereas proximal tubules were stained weak with the antigen. Immunostaining in glomeruler structures was changed from mild to weak. No staining was observed in endothelial cells of the capillaries (Figure 8A).

Group II. Immunostaining of caspase 3 antibody was noticed to change from weak to mild in proximal tubules and glomerules. Strong immunostaining was seen in distal tubules, whereas no staining was detected in endothelial cells (Figure 9A).

Group III. Immunostaining changed from weak to mild in proximal tubules and endothelial cells. Staining intensity was more pronounced in distal tubules. Glomerules were shown to have a mild immunoreaction (Figure 10A).

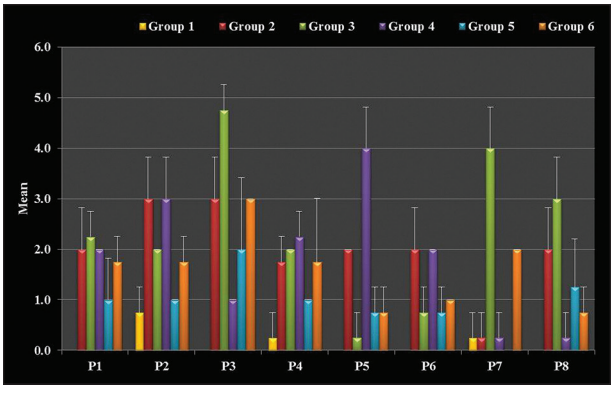

Figure 7 Mean of degeneration criteria in TEM. P1=electron-dense intramembranous deposits, P2=electron-dense mesangial deposits, P3=foot process effacement, P4=inclusions, P5=large vacuoles, P6=GBM thickening, P7=GBM curling, and P8=GBM deletion.

Table II *Degeneration Criteria in SEM*

Degeneration criterion	Group 1	2	3	4	5	6	p Value
Precipitated phthalate crystals	0.00 ± 0.00^{a}	2.17 ± 0.75^{b}	4.67 ± 0.52^{c}	0.33 ± 0.52^{a}	0.17 ± 0.41^{a}	1.50 ± 0.84^{b}	<0.001
Distortion in erythrocyte shape	0.00 ± 0.00^{a}	0.17 ± 0.41^{a}	2.00 ± 1.41^{b}	0.17 ± 0.41^{a}	0.00 ± 0.00^{a}	0.00 ± 0.00^{a}	0.002
Foot process effacement	0.00 ± 0.00^{a}	3.00 ± 1.55^{b}	4.83 ± 0.41^{c}	1.00 ± 0.89^{a}	0.33 ± 0.52^{a}	3.00 ± 0.60^{b}	<0.001
Distortion in podocyte shape	0.00 ± 0.00^{a}	2.00 ± 1.26^{b}	3.00 ± 0.63^{c}	$2.00\pm0.63^{b,c}$	0.17 ± 0.41^{a}	2.00 ± 0.00^{b}	<0.001

Data are given as mean±standard deviation.
[a,b,c]The difference between the averages indicated by different letters are statistically significant, while the difference between the averages indicated by the same letters are not statistically significant ($p<0.05$).

Group IV. Weak immunostaining was noticed in proximal tubules and endothelial cells. Glomerular immunostaining was changed from weak to mild, and immunostaining in distal tubules was changed from mild to strong (Figure 11A).

Group V. Proximal tubules, glomerules, and endothelial cells of capillaries were seen to have weak immunostaining with the antibody. Mild immunostaining was detected in the distal tubules (Figure 12A).

Group VI. Weak and mild immunoreactions were noticed in glomerules and endothelial cells, respectively. Mild to strong staining of caspase 3 was noticed in distal tubules, whereas this staining was observed to change from weak to mild in proximal tubules (Figure 13A).

The most pronounced immunostaining was seen in groups III and IV. These groups were followed by groups II and VI, respectively. The density of the reaction in group V was significantly less than that in groups II and VI ($p<0.05$). Group I showed weak immunoreactivity with caspase 3 antibody. Strong caspase 3 immunoreactivity was observed in distal tubules of the renal cortex. In terms of immunoreactivity, distal tubules were followed by the glomerulus and the proximal tubule. The weakest reaction was seen in endothelial cells. These results were statistically significant ($p<0.05$). A comparison of caspase 3 reaction density between groups is shown in Figure 14 and Table III. Mean of degeneration criteria in SEM is presented in Figure 15.

ET-1 Immunostaining

Immunohistochemistry was done for the detection of DBP-induced possible degeneration in the kidney by using polyclonal antibodies against ET-1 antigen.

Group I. Immunostaining in the control group was noticed to be weak in glomerules and endothelial cells, whereas it was mild in distal tubules. The intensity of reaction was seen to change from weak to mild in the proximal tubules (Figure 8B).

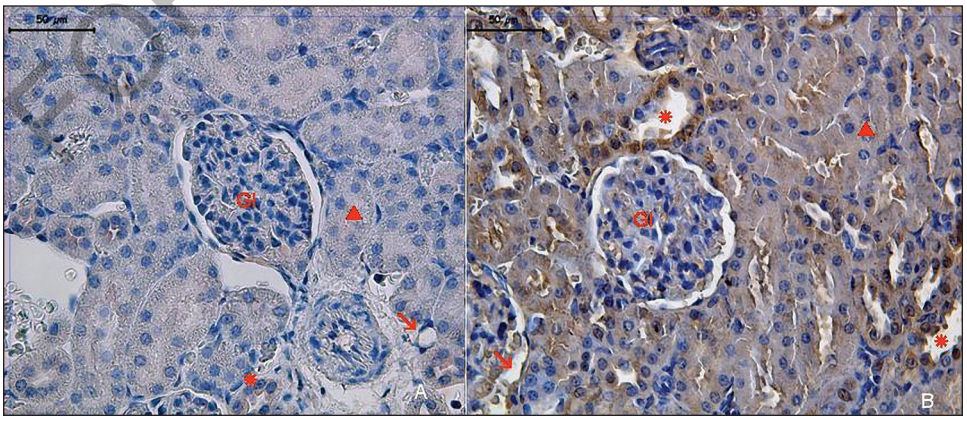

Figure 8
Expression of caspase 3 (A) and ET1 (B) are seen in glomerulus (Gl), proximal tubule (▲), distal tubule (✱), and endothelium (↘) of blood vessels.

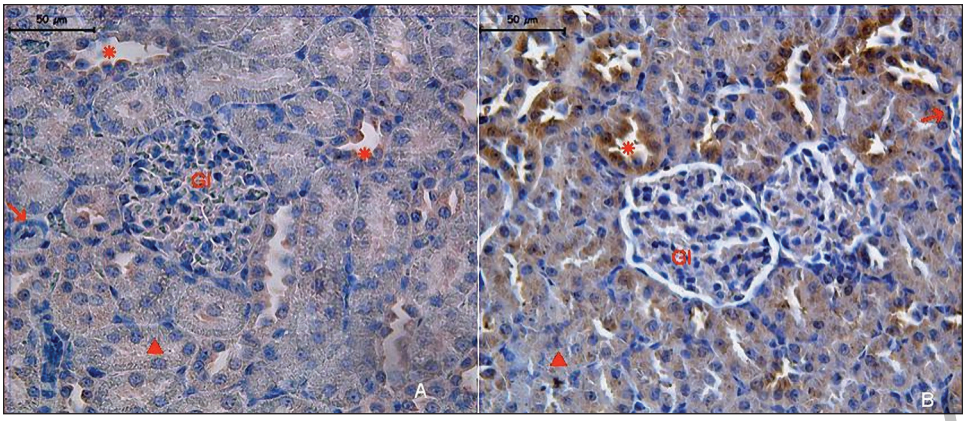

Figure 9
Expression of caspase 3 (A) and ET1 (B) are seen in glomerulus (Gl), proximal tubule (▲), distal tubule (✱), and endothelium (↘) of blood vessels.

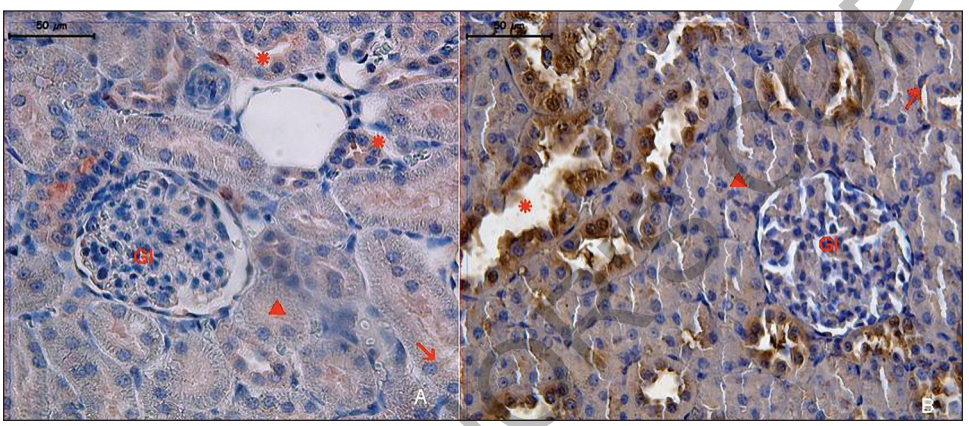

Figure 10
Expression of caspase 3 (A) and ET1 (B) are seen in glomerulus (Gl), proximal tubule (▲), distal tubule (✱), and endothelium (↘) of blood vessels.

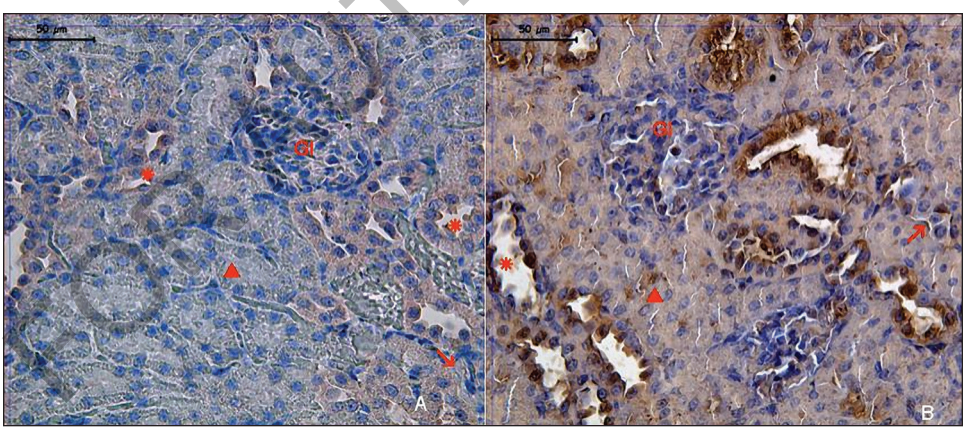

Figure 11
Expression of caspase 3 (A) and ET1 (B) are seen in glomerulus (Gl), proximal tubule (▲), distal tubule (✱), and endothelium (↘) of blood vessels.

Group II. Mild reaction in proximal tubules and weak reaction in endothelial cells were noticed in the low-dose–treated group. The most pronounced reaction was observed in the distal tubules. Immunostaining in glomerular structures was detected to change from weak to mild (Figure 9B).

Groups III and IV. Immunostaining intensity in the

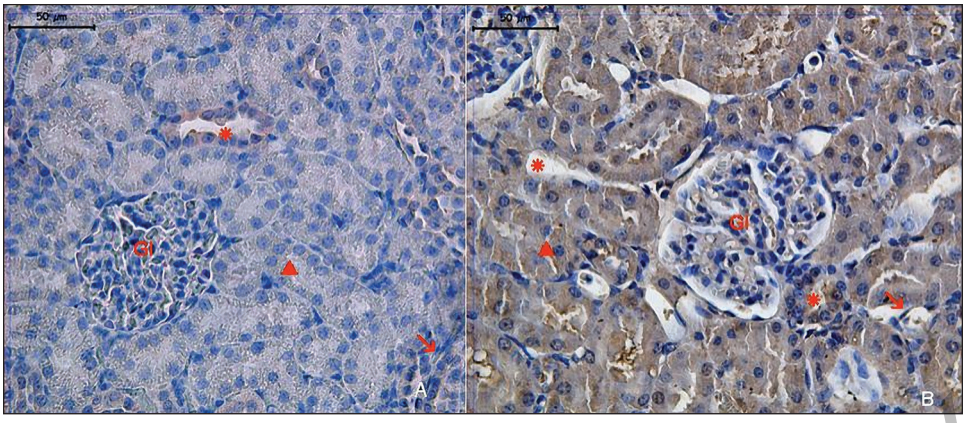

Figure 12
Expression of caspase 3 (A) and ET1 (B) are seen in glomerulus (Gl), proximal tubule (▲), distal tubule (✱), and endothelium (↘) of blood vessels.

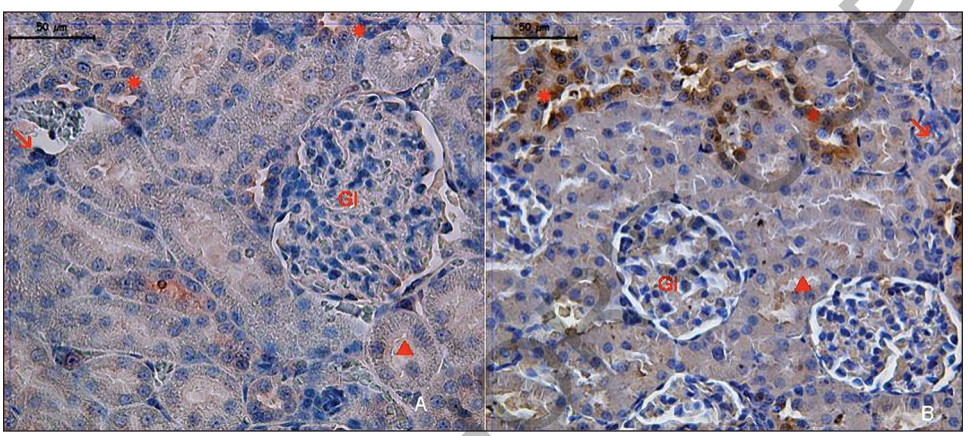

Figure 13
Expression of caspase 3 (A) and ET1 (B) are seen in glomerulus (Gl), proximal tubule (▲), distal tubule (✱), and endothelium (↘) of blood vessels.

cortical structures of kidney tissues was very similar in these groups. Distal tubules were detected to stain strongly positive. In proximal tubules immunoreaction was noted to change from mild to strong. Immunostaining of endothelial cells was observed to change from weak to mild. Glomerular structures had a mild immunoreaction in Group III, whereas it was observed to change from mild to strong in Group IV (Figures 10B and 11B).

Group V. ET-1 immunostaining detected in glomeruler structures and endothelial cells was weak, but it changed from weak to mild in proximal and distal tubules (Figure 12B).

Group VI. Mild immunoreaction was observed in proximal tubules and glomerular structures. ET-1 immunostaining was detected to change from mild to strong in distal tubules and from weak to mild in endothelial cells (Figure 13B).

The most prevalent and strong ET-1 staining was observed in groups III and IV. Compared to groups

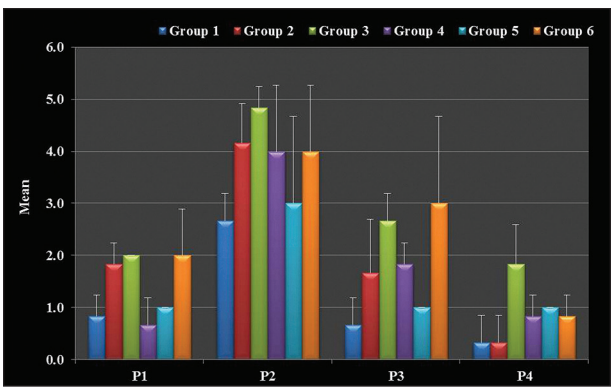

Figure 14 Evaluation of caspase-3 primary antibody intensity between groups. P1 = proximal tubule, P2 = distal tubule, P3 = glomerulus, P4 = endothelial capillary cells.

Table III *Evaluation of Caspase-3 Primary Antibody Intensity*

	Group						
Structure	**1**	**2**	**3**	**4**	**5**	**6**	**p Value**
Proximal tubule	$^{a}0.83 \pm 0.41^{a}$	$^{a}1.83 \pm 0.41^{b}$	$^{a}2.00 \pm 0.00^{b}$	$^{a}0.67 \pm 0.52^{c}$	$^{a}1.00 \pm 0.00^{c}$	$^{a,b}2.00 \pm 0.89^{b}$	<0.001
Distal tubule	$^{b}2.67 \pm 0.52^{a}$	$^{b}4.17 \pm 0.75^{b}$	$^{b}4.83 \pm 1.41^{b}$	$^{b}4.00 \pm 1.26^{a,b}$	$^{b}3.00 \pm 1.67^{a,b}$	$^{b}4.00 \pm 1.26^{a,b}$	0.034
Glomerulus	$^{a}0.67 \pm 0.52^{a}$	$^{a}1.67 \pm 1.03^{a,b}$	$^{a}2.67 \pm 0.52^{b}$	$^{a,b}1.83 \pm 0.41^{b}$	$^{a}1.00 \pm 0.00^{a}$	$^{b}3.00 \pm 1.67^{b}$	0.001
Endothelial cells of capillaries	$^{a}0.33 \pm 0.52^{a}$	$^{a}0.33 \pm 0.52^{a}$	$^{a}1.83 \pm 0.75^{b}$	$^{a}0.83 \pm 0.41^{a,b}$	$^{a}1.00 \pm 0.00^{a,b}$	$^{a}0.83 \pm 0.41^{a,b}$	0.002
p Value	0.002	0.002	0.002	0.001	0.002	0.006	

Data are given as mean ± standard deviation.
^{a,b,c}The difference between the averages indicated by different letters are statistically significant, while the difference between the averages indicated by the same letters are not statistically significant ($p < 0.05$).

III and IV, weak and mild immunoreactions were seen in groups I, II, and VI. Between these 3 groups the weakest immunoreaction was detected in group II. Group V showed the weakest immunoreaction of all the groups. These results were statistically significant in tubular and glomerular structures of kidney tissue ($p < 0.05$). A comparison of ET-1 reaction density between the groups is shown in Figure 16 and Table IV, and a general comparison of the intensity of primary antibodies (caspase 3/ET-1) is shown in Figure 17.

Malondialdehyde and Total Sulphydryl Group (RSH) Results

Malondialdehyde (MDA) concentrations in kidney tissues were used as a measure of LPO. Figure 18 and Table V show the results of MDA changes in all groups. The MDA concentrations were similar in the control and low-dose DBP + resveratrol groups ($p < 0.05$). Both high- and low-dose DBP and CMC administration induced a statistically significant increase in the formation of LPO as compared to the control group ($p < 0.05$). Treatment of rats with resveratrol in the low-dose DBP group reduced the MDA concentration more effectively than in the high-dose DBP group ($p < 0.05$).

Figure 19 and Table V show the results of the total sulphydryl group (RSH) changes in all groups. The RSH levels were similar in the controls and the low-dose DBP + resveratrol groups ($p < 0.05$). Administration of DBP significantly reduced RSH level as compared to that of the control group, and this was reduced more in the high-dose DBP group as compared with the low-dose DBP group ($p < 0.05$). Interestingly, the RSH levels in the CMC and low-dose DBP + resveratrol groups were very similar and were significantly reduced as compared to that of the control group ($p < 0.05$). Animals treated with resveratrol + high-dose DBP, as compared to the low-dose DBP + resveratrol group, exhibited a more

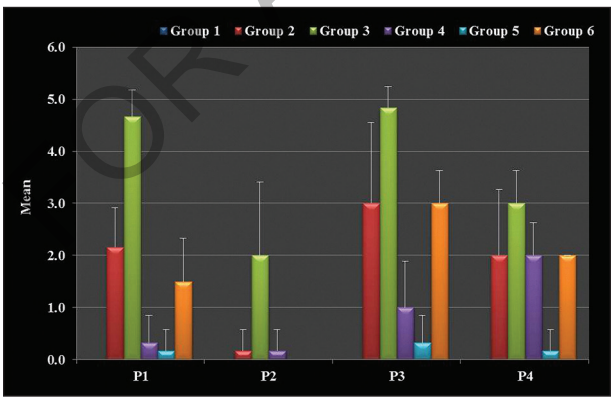

Figure 15 Degeneration criteria in SEM. P1 = precipitated phthalate crystals, P2 = distortion in erythrocyte shape, P3 = foot process effacement, and P4 = distortion in podocyte shape.

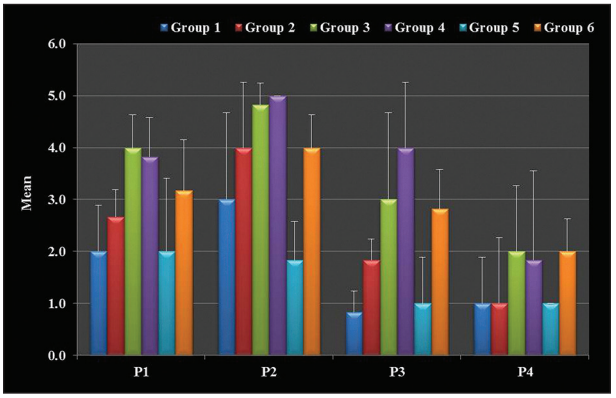

Figure 16 Evaluation of ET-1 primary antibody intensity between groups. P1 = proximal tubule, P2 = distal tubule, P3 = glomerulus, and P4 = endothelial capillary cells.

Table IV *Evaluation of ET-1 Primary Antibody Intensity*

	Group						
Degeneration criterion in SEM	**1**	**2**	**3**	**4**	**5**	**6**	**p Value**
Proximal tubule	[a]2.00±0.89[a]	[a,b]2.67±0.52[a]	[a]4.00±0.63[b]	[a,b]3.83±0.75[a,b]	2.00±1.41[a,b]	[a,b]3.17±0.98[a,b]	0.004
Distal tubule	[a,b]3.00±1.67[a,b]	[b]4.00±1.26[a,b]	[a]4.83±0.41[a]	[a]5.00±0.00[a]	1.83±0.75[b]	[b]4.00±0.63[a,b]	0.001
Glomerulus	[a,b]0.83±0.41[a]	[a,c]1.83±0.41[b]	[a,b]3.00±1.67[b]	[a,b]4.00±1.26[b]	1.00±0.89[a]	[a,c]2.83±0.75[b]	<0.001
Endothelial cells of capillaries	[b]1.00±0.89	[a,c]1.00±1.26	[b]2.00±1.26	[b]1.83±1.72	1.00±0.00	[a,c]2.00±0.63	0.275
p Value	0.017	0.009	0.007	0.009	0.098	0.006	

Red-colored letters show the significance in groups (significance of the differences, about 4 parameters for each group). Black-colored letters show the significance between groups.

significantly reduced RSH level. Therefore, resveratrol pretreatment could inhibit DBP-induced increase in kidney total sulphydryl groups (RSH).

Discussion

The available literature indicates that no previous studies have been done to evaluate the antioxidant capacity of resveratrol and its protective effect against DBP toxication in the kidney. Mechanisms of PAE-induced damage include a reduction of RSH level and result in the formation of degeneration and increasing apoptosis in kidney tissues.[23]

The present study concentrates on the possible protective effects of resveratrol on DBP-induced nephrotoxicity. Biochemical analysis was done for oxidative stress indices such as LPO level. The activity of antioxidants was measured with total sulphydryl groups (RSH) because that antioxidant is most commonly affected by DBP toxicity.[23] Histological changes of the kidney were examined by immunohistochemical and electron microscopic techniques.

In our study LPO level was significantly elevated in kidney tissues of rats treated with DBP as compared to those of the control group, thus suggesting increased oxidative stress ($p<0.05$). There have been no studies so far which sought to investigate DBP-caused damage in kidney tissues. In general, studies were carried out on other PAEs. Similar with our findings, significant LPO level elevation was reported in PAEs and cadmium-induced renal damage.[24,25]

In the present study the elevation in the free radicals (LPO) induced by DBP was significantly decreased in the presence of resveratrol, especially in the low-dose DBP+resveratrol group ($p<0.05$). A slight decrease of the LPO level occurred in the high-dose DBP+resveratrol group, but this increase was not as significant as that in the low-dose group ($p<0.05$). This finding suggests that resveratrol minimizes the toxic effect of DBP via its antioxidant activity. These results are in the line with the view held by Soares, who confirmed the role of resveratrol as an anti-

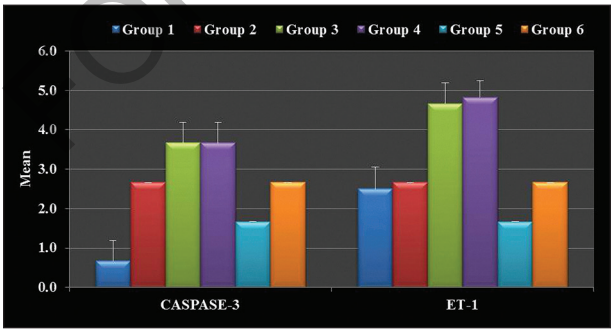

Figure 17 General comparison of the intensity of primary antibodies.

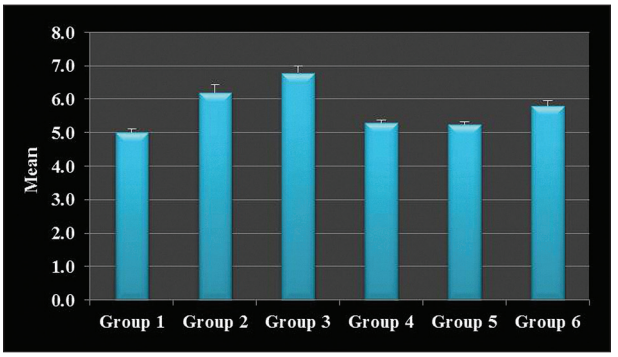

Figure 18 Mean of MDA levels.

Table V *MDA and RSH Changes Between the Groups*

Group	MDA (nmol/g)	RSH (nmol/g)
1	5.01 ± 0.11^{a}	0.52 ± 0.06^{a}
2	$6.21 \pm 0.22^{b,d}$	0.35 ± 0.03^{b}
3	6.80 ± 0.21^{b}	0.26 ± 0.01^{c}
4	5.30 ± 0.09^{c}	$0.47 \pm 0.04^{a,d}$
5	5.25 ± 0.07^{c}	0.46 ± 0.03^{a}
6	5.80 ± 0.14^{d}	$0.40 \pm 0.02^{b,d}$
p Value	<0.001	<0.001

Data are given as mean ± standard deviation.

oxidant agent in glycerol-induced renal injury.[9] Additionally, Kolgazi et al found that resveratrol reduced renal tissue damage by balancing oxidant-antioxidant levels.[11]

In agreement with a previous study, the level of RSH was significantly decreased in the plasma of both DBP-treated groups as compared to the control group ($p < 0.05$). This decrease was more prominent in the high-dose–treated DBP group, and this decrease in RSH level may be due to its consumption in the prevention of free radical–mediated lipid peroxidation.[26,27]

Furthermore, it has been suggested that the decrease in GSH and/or RSH levels upon DBP exposure might impair the degeneration of lipid peroxides, thereby leading to its accumulation in the target organs.[28]

Coadministration of resveratrol with low-dose DBP increased the level of antioxidants (RSH) and approximated to the normal values of the control group. While the high-dose resveratrol-treated group experienced a degree of RSH rise, this was not as noticeable as that seen in the low-dose DBP group ($p < 0.05$). There are many studies in the literature to support our findings about the effect of resveratrol on increasing antioxidant levels.[9-12,29]

PAE-induced nephrotoxicity has been discussed in many studies.[1-3,23,30,31] Fujimoto et al reported that nonylphenol (NP), as DBP-like PAEs, caused necrosis in proximal, distal, and collecting tubule epithelium.[30]

Epidemiological studies have revealed that DBP is one of the most toxic of the PAEs to humans. It is also a widespread environmental pollutant found in drinking water, hair spray, nail polish, and even toys, and therefore people are quite often confronted with it in daily life. This vast scale of exposure to contaminants accumulates and may cause serious damage in kidney tissues after intake to the body.[1,2,32]

In the present study, administration of low-dose DBP (500 mg/kg) for 30 days induced prominant damage in the structure of kidney glomerules, as assessed by the existence of electron (e–)–dense intramembranous and mesangial deposition, foot process effacement, accumulation of inclusions, and existence of large vacuoles in both mesangial cells and podocytes, and different kinds of GBM degenerations in TEM. These findings were more severe in the high-dose DBP-treated group. To date, there have been no studies showing the glomerular damage caused by DBP at the ultrastructural level. However, studies have reported similar degenerative changes on glomeruli caused by other PAEs and heavy metals such as cadmiums.[3,23,30,31] Our evaluation with SEM has demonstrated similar findings: that is, the highest-dose DBP-treated group displayed more severe degenerative changes in the precipitation of phthalate crystals, foot process effacement, and distortion in the shape of the podocytes and erythrocytes as compared to the low-dose DBP-treated group ($p < 0.05$). Likewise, while there have been no SEM studies in the literature investigating DBP-induced glomerular damage, studies have demonstrated that different PAEs and heavy metals cause degenerative changes in SEM. Evan et al reported glomerular damage arising from glomerular perfusion similar with our results, showing epithelial foot process effacement and fusion in the epithelial foot processes.[33] Bohle et al examined the glomerular structure in human acute renal failure using TEM and SEM; however, their findings were different from those of our study and other studies in the literature as they reported that the

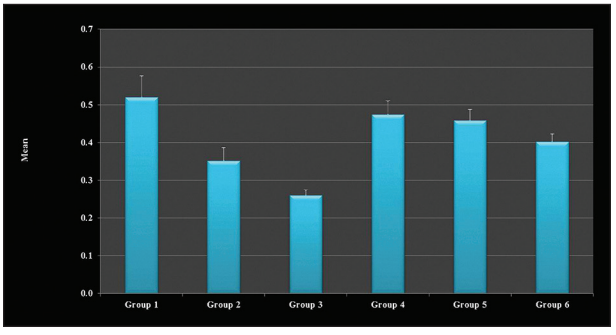

Figure 19 Mean of total sulphydryl group (RSH) levels.

structures of podocytes were not much different from those of the control group.[34] In another study, folic acid–treated glomeruli were investigated with SEM, and deposits of precipitated crystals were observed on the surfaces of podocytes, correlating with the findings of our DBP groups.[35]

In the resveratrol-treated groups, ultrastructural degenerative findings observed with TEM-SEM evaluations of both solvent and DBP-treated groups also significantly recovered. A remarkable result of our study is that the CMC that was used as a solvent for resveratrol resulted in significant degenerative findings in the renal cortex ($p<0.05$). However, it was also demonstrated that resveratrol could reverse the renal cortical damage due to the CMC and DBP ($p<0.05$). When there was a similar regeneration in the low-dose DBP+resveratrol group and the control group, the structural improvement seen in the high-dose DBP+resveratrol group was noted to be less as compared to that of the control group ($p<0.05$).

This study seeks to evalute DBP-induced potential renal cortical damage using caspase 3 and ET-1 antibodies. Immunohistochemistry has demonstrated that the strongest level of immunoreactivity was seen in high-dose DBP- and CMC-treated groups as evidenced by results with both ET-1 and caspase 3 ($p<0.05$) (Table VI). The low-dose DBP group was shown to have a weaker immunoreactivity. The caspase 3 expressed in the latest stages of apoptosis exhibited the most intense reaction in distal tubules. Caspase 3 reaction was noted to be gradually reduced in the glomeruli, proximal tubule, and endothelial cells, respectively ($p<0.05$). This suggested that the enhancing effect of DBP on apoptosis occurred mainly in distal tubules and glomeruli. Another study with a study design similar to ours has reported that in the presence of renal tubular damage, distal tubule epithelial cells show the strongest reaction to caspase 3, whereas proximal tubules and glomeruli mostly stain negative.[36] Bamri-Ezzine et al investigated the tubular epithelial cell apoptosis in glycogen nephrosis of diabetes mellitus and similarly observed the dense immunoreactivity with caspase 3 in the distal tubular cells.[37]

ET-1 expression is immunopositive in distal and proximal tubules of normal kidney tissue. However, increased ET-1 expression has been reported in various tissues, including those in the kidney, as a result of experimentally-induced or chemically-induced damage.[16] In our study ET-1 expression in whole kidney tissue was seen to rise significantly in both the high-dose and low-dose DBP groups, whereas this was more prominent in the high-dose group ($p<0.05$). The most obvious and strongest immunostaining was observed in the distal tubular epithelial cells ($p<0.05$). There was also an increased expression in the proximal tubules, glomeruli, and endothelial cells as compared to those of the control group ($p<0.05$). Therefore, it is most likely that the degenerative changes in the renal cortex mostly occurred in the distal tubules, followed by glomeruli, proximal tubule, and endothelial cells. While there are no immunohistochemical studies in the literature investigating DBP-induced renal cortical damage using ET-1 antibody, studies searching for renal damage induced under experimental conditions or caused by various pathological conditions have established findings similar to those of our study, showing increased ET-1 expression in distal renal tubules.[38,39]

Similar to the electron microscopy results, a significant reduction of reaction intensity was seen in caspase 3 and ET-1 immunostaining of the low-dose DBP+resveratrol group (Table VI). However, the amount of this reduction was not significant in the high-dose DBP+resveratrol group as compared to the low-dose group ($p<0.05$). This result has demonstrated that resveratrol yields more expected outcomes in the prevention of renal cortical apoptosis and reversal of degenerative changes in the low-dose DBP group as compared to the high-dose DBP group ($p<0.05$).

In conclusion, the present study highlights the outcomes of resveratrol administration in combination with high- and low-dose DBP exposure. A minimization of hazards was seen especially in the low-dose DBP group. Resveratrol as used in our study can protect the tissues against oxida-

Table VI *General Comparison of the Intensity of Primary Antibodies*

	Antibody	
Group	**Caspase-3**	**ET-1**
1	0.67 ± 0.52^{a}	2.50 ± 0.55^{a}
2	$2.67\pm0.52^{b,c}$	$2.67\pm0.52^{a,b}$
3	3.67 ± 0.52^{c}	4.67 ± 0.52^{c}
4	3.67 ± 0.52^{c}	4.83 ± 0.41^{c}
5	$1.67\pm0.52^{a,b}$	$1.67\pm0.52^{a,b}$
6	$2.67\pm0.52^{b,c}$	$2.67\pm0.52^{a,b}$
p Value	<0.001	<0.001

Data are given as mean±standard deviation.

tive stress induced by DBP via both lowering the amount of free radicals and increasing the level of antioxidants. Further studies are needed to better understand the use of resveratrol and its therapeutic potential in humans. Several antioxidant analyses were performed for the evaluation of chemical and biological functions of resveratrol. In addition, considering the sources of DBP in food, water, and personal-care products, attention should be paid to reduce exposure to DBP. Furthermore, a diet rich in resveratrol could be beneficial to reducing the toxicity of DBP.

Acknowledgments

We would like to thank Ms. Canan Zaimoğlu for her valuable assistance in preparing the manuscript. We would like to thank Bulent Celik, Associate Professor, Department of Statistics, Faculty of Sciences, Gazi University, for his assistance with the statistics and tables in this article.

References

1. Liao C, Chen L, Chen B, Lin S: Bioremediation of endocrine disruptor di-n-butyl phthalate ester by Deinococcus radiodurans and Pseudomonas stutzeri. Chemosphere 2010;78: 342-346
2. Saillenfait AM, Sabate JP, Gallissot F: Developmental toxic effects of diisobutyl phthalate, the methyl-branched analogue of di-n-butyl phthalate, administered by gavage to rats. Tox Let 2006;165:39-46
3. Wu X, Wang Y, Liang R, Dai Q, Jin D, Chao W: Biodegradation of an endocrine-disrupting chemical di-n-butyl phthalate by newly isolated Agrobacterium sp. and the biochemical pathway. Process Biochem 2011;46:1090-1094
4. Rozati R, Reddy P, Reddanna P, Mujtaba R: Role of environmental estrogens in the deterioration of male factor fertility. Fertil Steril 2002;78:1187-1194
5. Hostetter T, Olson J, Rennke H, Venkatachalam M, Brenner B: Hyperfiltration in remnant nephrons: A potentially adverse response to renal ablation. Renal Physiol 1981;241:85-93
6. Kavlock R, Boekelheide K, Chapin R, Cunningham M, Faustman E, Foster P, Golub M, Henderson R, Hinberg I, Little R, Seed J, Shea K, Tabacova S, Tyl R, Williams P, Zacharewski T: NTP Center for the evaluation of risks to human reproduction: Phthalates expert panel report on the reproductive and developmental toxicity of di-n-butyl phthalate. Reprod Toxicol 2002;16:489-527
7. Fukui M, Yamabe N, Zhu BT: Resveratrol attenuates the anticancer efficacy of paclitaxel in human breast cancer cells in vitro and in vivo. Eur J Cancer 2010;46:1882-1891
8. Palsamy P, Subramanian S: Resveratrol protects diabetic kidney by attenuating hyperglycemia-mediated oxidative stress and renal inflammatory cytokines via Nrf2-Keap1 signaling. Biochim Biophys Acta 2011;1812:719-731
9. Soares TJ, Volpini R, Francescato H, Costa R, Silva C, Coimbra T: Effects of resveratrol on glycerol-induced renal injury. Life Sci 2007;81:647-656
10. Saito M, Satoh S, Kojima N, Tada H, Sato M, Suzuki T, Senoo H, Habuchi T: Effects of a phenolic compound, resveratrol, on the renal function and costimulatory adhesion molecule CD86 expression in rat kidneys with ischemia/reperfusion injury. Arch Histol Cytol 2005;68:41-49
11. Kolgazi M, Şener G, Çetinel Ş, Gedik N, Alican İ: Resveratrol reduces renal and lung injury caused by sepsis in rats. J Surg Res 2005;134:315-321
12. Porter A, Janicke R: Emerging roles of caspase-3 in apoptosis. Cell Death Differ 1999;6:99-104
13. Yang B, El Nahas AM, Thomas GL, Haylor JL, Watson PF, Wagner B, Johnson TS: Caspase-3 and apoptosis in experimental chronic renal scarring. Kidney Int 2001;60:1765-1776
14. Cummings B, Schnellmann RG: Cisplatin-induced renal cell apoptosis: Caspase3-dependent and independent pathways. J Pharmacol Exp Ther 2002;302:8-17
15. Yang B, Johnson TS, Thomas GL, Watson PF, Wagner B, Nahas ME: Apoptosis and Caspase-3 in experimental anti-glomerular basement membrane nephritis. J Am Soc Nephrol 2001;12:485-495
16. Lee J, Hung C, Tsai J, Chen H: Endothelin-1 enhances superoxide and prostoglandin E2 production of isolated diabetic glomeruli. J Med Sci 2010;26:350-356
17. Mahood KI, McKinnel C, Walker M, Hallmark N, Scott H, Fisher JS, Rivas A, Hartung S, Ivell R, Mason JI, Sharpe RM: Cellular origins of testicular dysgenesis in rats exposed in utero to di(n-butyl) phthalate. Int J Androl 2005;29:148-154
18. Sharma S, Anjaneyulu M, Kulkarni SK, Chopra K: Resveratrol, a polyphenolic phytoalexin, attenuates diabetic nephropathy in rats. Pharmacology 2006;76:69-75
19. Zhang XF, Zheng J, Li Z, Zhang Y: Glucocorticoid pathway mediated the inhibition of testosteron in rats exposed to dibutyl phthalate. Zhonghua Yu Fang Yi Xue Za Zhi 2009;8: 710-713
20. McCarty KS, Miller LS, Cox EB, Konrath J: Estrogen receptor analysis: Correlation of biochemical and immunohistochemical methods using monoclonal antireceptor antibodies. Arch Pathol Lab Med 1985;109:716-721
21. Kurtel H, Granger D, Tso P, Grisham MB: Vulnerability of intestinal fluid to the oxidant stress. Am J Physiol 1992;263: 573-578
22. Daniel WW: Biostatistics: A Foundation for Analysis in the Health Sciences. Eighth edition. New York, John Wiley & Sons, 2005, pp 000-000
23. Kavlock R, Boekelheide K, Chapin R, Cunningham M, Faustman E, Foster P, Golub M, Henderson R, Hinberg I, Little R, Seed J, Shea K, Tabacova S, Tyl R, Williams P, Zacharewski T: NTP Center for the evaluation of risks to human reproduction: Phthalates expert panel report on the reproductive and developmental toxicity of di-n-butyl phthalate. Reprod Toxicol 2002;16:489-527
24. Maier EA, Matthews RD, McDowell JA, Walden RR, Ahner BA: Environmental cadmium levels increase phytochelatin and glutathione in lettuce grown in a chelator-buffered nutrient solution. Environ Qual 2003;32:1356-1364
25. Jahangir T, Khan TH, Prasad L, Sultana S: Allevation of free

radical mediated oxidative and genotoxic effects of cadmium by farnesol in Swiss albino mice. Redox Rep 2005;6:303-310

26. Demopoulos H: Control of free radicals in biological system. Fed Proc 1973;32:1903-1908
27. Koyuturk M, Yanardag R, Bulken S, Tunali S: Influence of combined antioxidants against cadmium induced testicular damage. Environ Toxicol Pharmacol 2006;21:235-240
28. Sarkars S, Poonam Y, Bhatnagar D: Cadmium-induced lipid peroxidation and antioxidant enzymes in rat tissues: Role of vitamin E and selenium. Trace Elem Electro 1997;14:41-45
29. Al-Waili N: Effects of daily consumption of honey solution on hematological indices and blood levels of minerals and enzymes in normal individuals. J Med Food 2003;2:894-897
30. Fujimoto Y, Usa K, Sakuma S: Effects of endocrine disruptors on the formation of prostaglandin and arachidonoyl-CoA formed from arachidonic acid in rabbit kidney medulla microsomes. Prostoglandins Leukot Essent Fatty Acids 2005; 73:447-452
31. Tsutsumi T, Ichihara T, Kawabe M, Yoshino H, Asamoto M, Suzuki S, Shirai T: Renal toxicity induced by folic acid is associated with the enhancement of male reproductive toxicity of di(n-butyl) phthalate in rats. Reprod Toxicol 2004; 18:35-42
32. Lars J: Cadmium overload and toxicity. Nephrol Dial Transplant 2002;17:35-39
33. Evan AP, Gattone VH 2nd, Filo RS, Leapman SB, Smith EJ, Luft FC: Glomerular endothelial injury related to renal perfusion: A scanning electron microscopic study. Transplantation 1983;35:436-441
34. Bohle A, von Gise H, Schubert B, Wehrmann M, Mikeler E, Neuhaus G, Späth U: Transmission and scanning electron microscopy investigations on the structure of the ultrafilter of glomeruli in human acute renal failure. Am J Nephrol 1988;8:112-117
35. Jermanovich N, Jones DB, Spitzer R: SEM of complement-independent nephrotoxic nephritis. Scan Electron Microsc 1980;3:365-371
36. Yang F, Liu GS, Lu XY, Kang JL: [Expression of caspase-3 in rat kidney with renal tubular damage induced by lipopolysaccharide and hypoxia]. [Article in Chinese]. Nan Fang Yi Ke Da Xue Xue Bao 2009;29:2091-2093
37. Bamri-Ezzine S, Ao ZJ, Londoño I, Gingras D, Bendayan M: Apoptosis of tubular epithelial cells in glycogen nephrosis during diabetes. Lab Invest 2003;83:1069-1080
38. Shiraishi N, Kitamura K, Kohda Y, Narikiyo T, Adachi M, Miyoshi T, Iwashita K, Nonoguchi H, Miller RT, Tomita K: Increased endothelin-1 expression in the kidney in hypercalcemic rats. Kidney Int 2003;63:845-852
39. Wesson DE, Dolson GM: Endothelin-1 increases rat distal tubule acidification in vivo. Am J Physiol 1997;273(4 Pt 2): F586-F594